International Journal of Applied Power Engineering (IJAPE)
Vol. 13, No. 1, March 2024, pp. 1~10
ISSN: 2252-8792, DOI: 10.11591/ijape.v13.i1.pp1-10

Novel differential power processing technique for uneven partial shading mitigation in PV systems

Subhash Murkute[1], Vandana Abhay Kulkarni (Deodhar)[2]
[1]Department of Electrical Engineering, P.E.S. College of Engineering, Aurangabad, India
[2]Department of Electrical Engineering, Government College of Engineering, Aurangabad, India

Article Info

Article history:

Received Mar 4, 2023
Revised May 1, 2023
Accepted May 7, 2023

Keywords:

Conversion efficiency
Differential power processing
Mismatch loss
Partial shading
Submodule level differential power processing

ABSTRACT

Photovoltaic (PV) system output power greatly depends on environmental operating conditions. Partial shaded condition (PSC) operates PV string under mismatch. PV module mismatch has been one of the major causes for reduced amount of output power. Maximizing the amount of energy extraction from PV system under mismatch greatly influenced by conversion efficiency as well as the mismatch mitigation topology used. Differential power processing (DPP) is one of the advanced techniques to deal with mismatch conditions and enhance power output from a PV system. In this paper hybrid modular DPP topology is presented. The proposed technique mitigates the effect of mismatches at submodule and enhance power extraction from PV string. Since in majority shading on a PV module is nonuniform. The conversion efficiency of module level DPP shading mitigation techniques enhanced using submodule level DPP architecture. To demonstrate its applicability simulation study is carried out in MATLAB Simulink and results are compared with traditional bypass method and module level DPP. Simulation results showed the reduction in mismatch loss and improvement in efficiency and power output.

Corresponding Author:

Subhash Murkute
Department of Electrical Engineering, P.E.S. College of Engineering
Aurangabad, Maharashtra 431002, India
Email: murkutes@rediffmail.com

1. INTRODUCTION

The non-convectional energy sources play an important role in meeting the future energy demands. Due to the affluence of sunlight everywhere on earth surface solar photovoltaic (PV) is the most used RE source among all various RE technologies and is considered a very providential source of future electrical power generation [1], [2]. In PV system, series parallel connections of PV elements are required to match the load or interface parameters [3], [4]. The PV element may be cell, submodule or module. A group of series connected cells in a module called a submodule, and generally 2-5 submodules are there in a module. PV elements in a connected in series generates same amount of current operating under uniform irradiance and P-V and I-V characteristics had only one power peak (MPP). Mismatch in series string due to internal or external means results in reduced output power of entire string. Partial shading is one of the main causes of mismatch [5]. As a result, some portion of generated power get lost either within shaded PV element or due to bypass diodes. Also, activation of bypass diodes generates multiple peaks in P-V characteristics with one global MPP (GMPP) as in Figure 1. Under uneven irradiance the bypass diode of shaded module from PV string in Figure 1(a) activates and the resulted P-V characteristics is given by curve 2 Figure 1(b).

Various PV system configurations proposed to maximize the power output by reducing the mismatch losses using power electronics-based solutions, classified as full power processing (FPP) and differential power

processing (DPP) [6], [7] shown in Figure 2. The basic principle used is to operate each module at its MPP. In FPP, each PV element is operated at its MPP using DC-DC converters or microinverters Figures 2(a) and 2(b). These techniques improve power output, but has poor power conversion efficiency since full power is processed at all time. Also the converter power rating should be equal to PV element [7], [8].

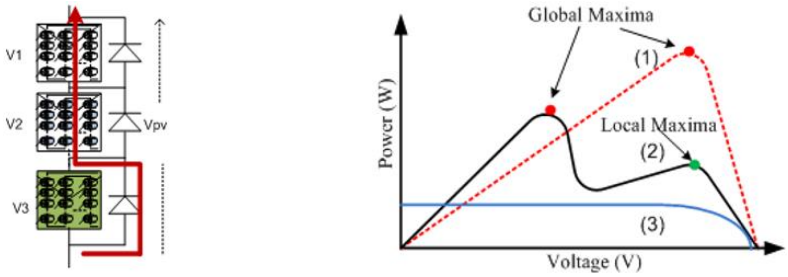

Figure 1. PV module array (a) series connection with bypass diode and (b) P-V characteristic

Recently differential power processing (DPP) techniques have been proposed, with improved conversion efficiency by processing a fraction of total power, only during mismatch condition in PV string [8], [9]. DPP techniques can reduce converter rating, size and cost, which mitigate mismatch at module level or submodule level. Series DPP architectures are categorized as: PV connected to PV (PV to PV), PV connected to bus (PV to bus) and PV to isolated bus (PV to IB) [6], [9], [10] Figures 2(c)-2(e) respectively. DPP converter used here provide the bypass path for mismatch current among PV elements and reduce the hotspot problem. PV module usually consists number of series connected PV submodules with bypass diodes. Module level mitigation methods reduce the effects of mismatching, but may not always prevent the activation of bypass diode at submodule level, which results in reduced power output from module. Since, in partially shaded PV module, the shaded submodule determines PV module current, drawn from the terminals of PV module, hence unshaded submodules and the whole PV string will be operating below their optimum power [11], [12]. DPP topologies using variety of DPP converters at submodule level are developing rapidly to overcome small level mismatch within the module to enhance power output capability [3], [10], [13]–[21]. These techniques improve the output from PV system using equal number of DPP converters as substrings in each module, raises to increased system cost and complexity. In [15] resonant switched-capacitor (ReSC) converter used in parallel at the sub-module level. Its conversion efficiency is 99% with low insertion loss but requires two switches per submodule. Simple energy recovery scheme presented in [8], uses combination of BBB and switched capacitor (SC) converters at panel level, requires minimum components, high efficiency, and simple control requirements. But it has two limitations i) Requires extra interconnecting DPP converter to interconnect two groups four PV modules and ii) Switches operates under hard switching increases losses. These limitations are overcome in [22], where BBB and ReSC converters are used. To reduce the control complexity and cost, majority of DPP topologies uses voltage equalization (VE) technique. Also, it doesn't require communication among the DPP converters [23].

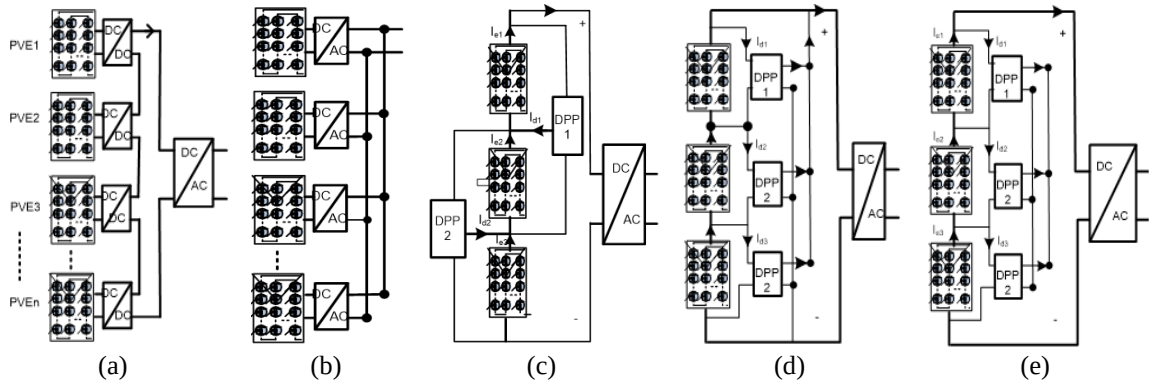

Figure 2. Mismatch mitigation techniques of (a) cascaded DC-DC converter (DCO), (b) microinverter, (c) PV to PV, (d) PV to bus, and (e) PV to isolated bus

This paper will propose simple DPP topology applied at both submodule and module level. It uses hybrid DPP architecture both PV to PV and PV to bus. Combination of bidirectional buck boost (BBB) and resonant switched capacitor (ReSC) converters are used [20]. It requires only one switch per submodule. The proposed architecture is easy to control, cost effective, highly efficient, modular and scalable. The paper is organized as in section 2 proposed DPP scheme is presented. Simulation results are presented in section 3 with considering various mismatch conditions. In section 4 conclusions are presented.

2. PROPOSED SUBMODULE LEVEL DPP ARCHITECTURE

Figure 3 show block diagram of proposed DPP architecture at submodule and module level of PV string of grid connected PV system with central MPPT control as well as standalone system. In this technique combination of bidirectional buck boost (BBB) converter and Resonant switch capacitor converter (ReSC) are used as DPP converters. BBB is used at SM level and ReSC at module level. Simple voltage balancing technique is used to operate each submodule at its MPP. These converters are active only during mismatch. Here it is assumed that each PV module consists of two submodules connected in series form one group. Circuit operation can be better described considering initially each converter working individually as follows.

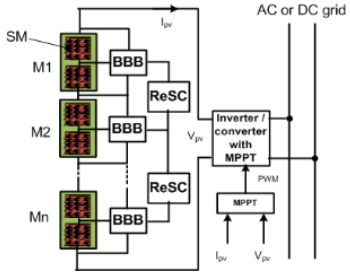

Figure 3. Proposed DPP architecture

2.1. Working principle

In proposed submodule level DPP architecture PV module is assumed to have two submodules (SM) forms one group and such two submodule groups (two PV modules) forms another group. BBB converter is used to compensate the mismatching between two submodules within a group. The ReSC is used to compensate the mismatch within a group of two PV modules. Two mismatch cases are considered: in first case mismatch is assumed between submodules of one module and in second case the mismatch between two neighboring modules is considered. The working principle of proposed submodule level DPP architecture is explained in following subsections.

2.1.1. Case 1: operation under uneven shading on submodules within one module

Figure 4 show mismatch mitigation within group of submodules. The substrings associated within group consists of submodules SM1 and SM2 connected to BBB converter Figure 4(a). This converter compensates the mismatch current between two neighboring submodules within the module. The value of inductor L and C is determined from (1) and (2) respectively.

$$L = \frac{D\,V_{oc}}{2\,f_S \Delta I_L} \quad (1)$$

$$C = \frac{D}{8\,f_S^2 L\,\Delta V} \quad (2)$$

Where ΔIL and ΔV are ripple in inductor current and string output voltage, fs is switching frequency, D duty ration and Voc open circuit module voltage. Consider SM1 is shaded and SM2 is operating at its full irradiance, hence Ism2 > Ism1. The circuit cycle of operation within the module is discussed in steps.

For step 1 operation S_2 is turned ON and S_1 OFF Figure 4(b). The mismatch current I_{sm2}-I_{sm1}=I_L flows through L and S_2. Current in inductor increases linearly and part of energy from fully irradiated SM2 temporarily stored in it. In second step, switch S_2 turned OFF and S_1 ON conducting reversely trough body diode as in Figure 4(c) and release the stored energy from L to load to compensate the current (I_{s1}) of shaded submodule (SM1). Since switches are operated at fixed duty cycle of 0.5, both the switch average current is half of the average inductor current I_L. The module current I_{m1} is supplied to load from M1 is calculated by writing KCL equations at X and Y nodes.

$$KCL\ at\ X: I_{m1} = I_{sm1} + I_{s1} \qquad KCL\ at\ Y: I_{m1} = I_{sm2} - I_{s2} \tag{3}$$

But $I_{s1} = I_{s2} = I_L/2$, hence:

$$I_{m1} = \frac{I_{sm1}+I_{sm2}}{2} \tag{4}$$

from (4), load current (IMPPT) is supplied from shaded as well as unshaded SM. The energy from shaded module is (SM2) is recovered and transferred to load, results in increased energy yield. With bypass diode technique, energy from shaded SM is zero.

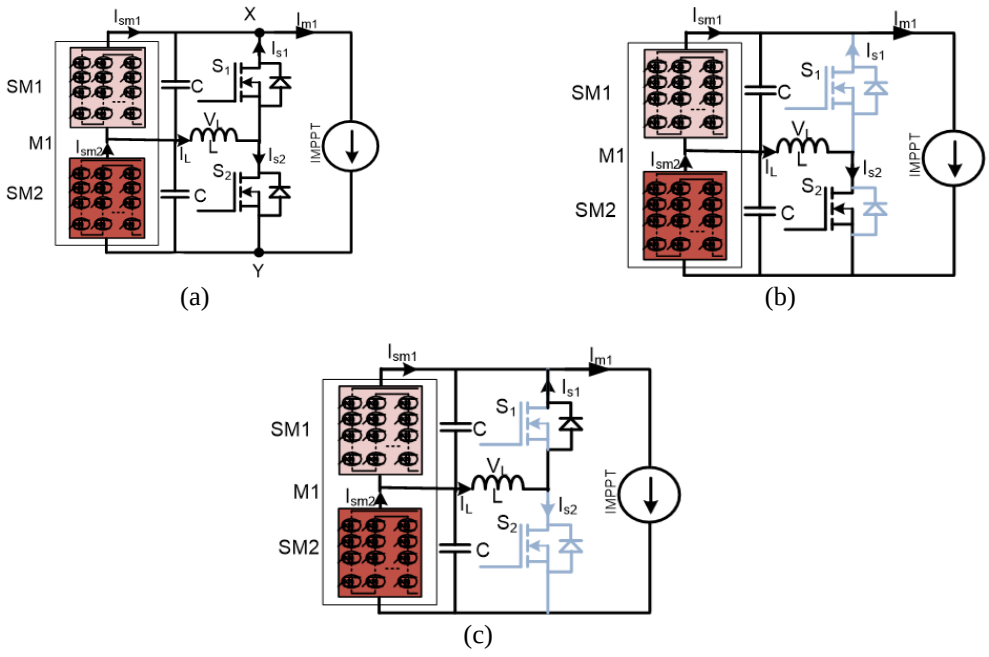

Figure 4. Mismatch mitigation of (a) BBB converter connection, (b) step 1 operation, and (c) step 2 operation

2.1.2. Case 2: operation under uneven shading between neighboring modules

Figure 5 show mismatch mitigation between two modules. Two submodules of one module considered as a one group. Group M1 formed by two submodules of module M1 and group M2 formed by two submodules of module M2. The mismatch mitigation between two groups M1 and M2 is handled by ReSC as in Figure 5(a). Assume group M1 submodules are shaded and group M2 unshaded. The current $I_{m1}<I_{m2}$ and voltages of M1 and M2 are $V_{M1}<V_{M2}$, where $V_{M1}=V_{sm1}+V_{sm2}$ and $V_{M2}=V_{sm3}+V_{sm4}$ and V_{sm1}, V_{sm2}, V_{sm3}, V_{sm4} submodule voltages. Now the mismatch power is processed through ReSC, and supplied to load. To understand this operation BBB converter is removed since only ReSC converter is involved in this operation and is explained in steps. Values of resonant converter components L_r and C_r selected using (5).

$$f_r = \frac{1}{2\pi\sqrt{L_r C_r}} \tag{5}$$

Where f_r is resonant frequency.

In step 1 switches S_2 and S_4 are simultaneously turned ON where as S_1 and S_3 are turned OFF. S_2 is conducting reversely through body diode as in Figure 5(b). Capacitor (C_r) start charging and energy from unshaded module (M2) get temporarily stored in it. In step2, switches S_1 and S_3 are turned ON where as S_2 and S_4 are turned OFF simultaneously Figure 5(c). The capacitor gets discharged and stored energy get released to load and the MPP current derived similar to BBB converter given as (4).

$$I_{PV} = \frac{I_{M1}+I_{M2}}{2} \tag{6}$$

The (6) shows that the MPP current is contributed by both shaded and nonshaded module and hence improves energy yield. Each DPP converters are operated at 50% duty ratio, therefore the submodule voltages get equalized during mismatch.

$V_{sm1}d_1 = V_{sm2}d_2$ where $d_1 = d_2 = 0.5$ duty ratio of DPP, hence $V_{sm1} = V_{sm2}$

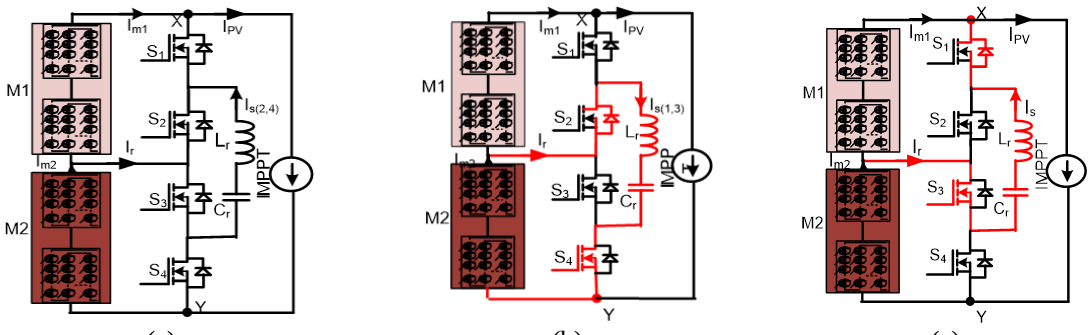

Figure 5. ReSC operation using (a) ReSc connections, (b) step 1 operation, and (c) step 2 operation

3. SIMULATION STUDY AND PERFORMANCE ANALYSIS

The proposed hybrid mismatch mitigation is validated using MATLAB Simulink simulation is shown in Figure 6. A 1 kW PV system, having four series connected PV modules are used. Each module has maximum power output of 250 W at STC of 1000 W/m^2 and 25 °C. Other parameters used in simulation model are given in Table 1. The proposed system practical applicability is tested for different shading conditions in Figure 7. These shading conditions are considered for naturally occurring shading events such as dust accumulation, bird dropping, clouding, tree shading, overhead wires, and or tall building nearby. Irradiance levels of PV module or submodules for these shading events are given in Table 2. System output performance is verified for different partial shading conditions as given in Figure 7 and compared with theoretical, bypass diode and module level DPP techniques.

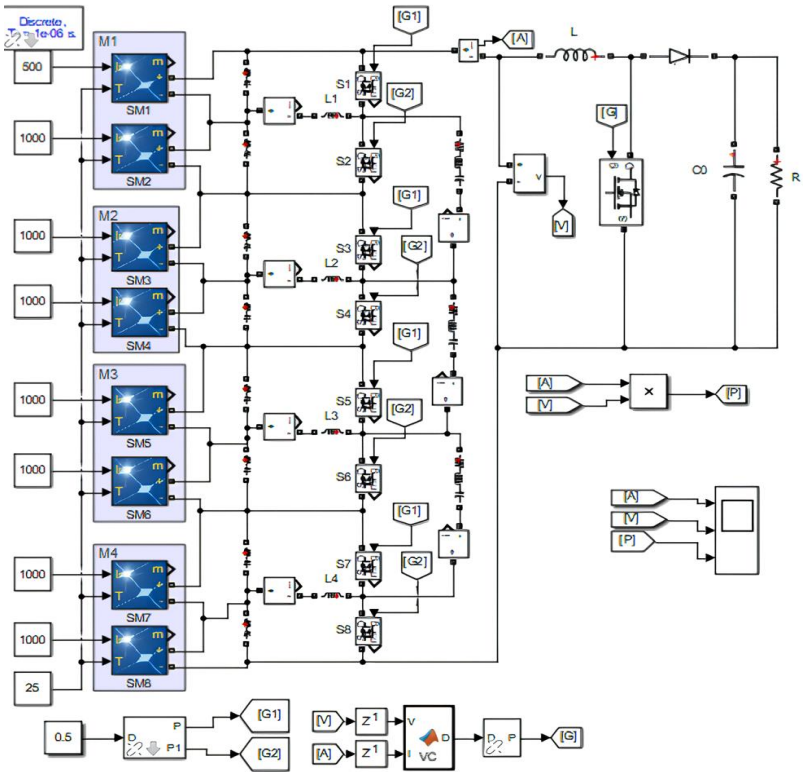

Figure 6. Simulation model of proposed PV system

Table 1. Simulation model parameters

S.N.	Model element	Parameter value
1	PV module	Series cells:60; Pm=250 W; Voc=37.8 V; Isc=8.56 A, Imp=8.06 A; Vm=31 V
2	L_1=L_2	0.2 mH
3	C_1=C_2=C_3=C_4	470 µF
4	L_r	1 µH
5	C_r	10 µF
6	f_s	50 kHz
7	d_1=d_2	0.5

Table 2. Irradiance level for shading events

S.L.	Shading event	Irradiance level (W/m^2)
1	Dust accumulation	500-800
2	Tree shade	400-600
3	Bird dropping	100-300
4	Clouding	200-700
5	Overhead wire	300-700
6	Tall building	200-500

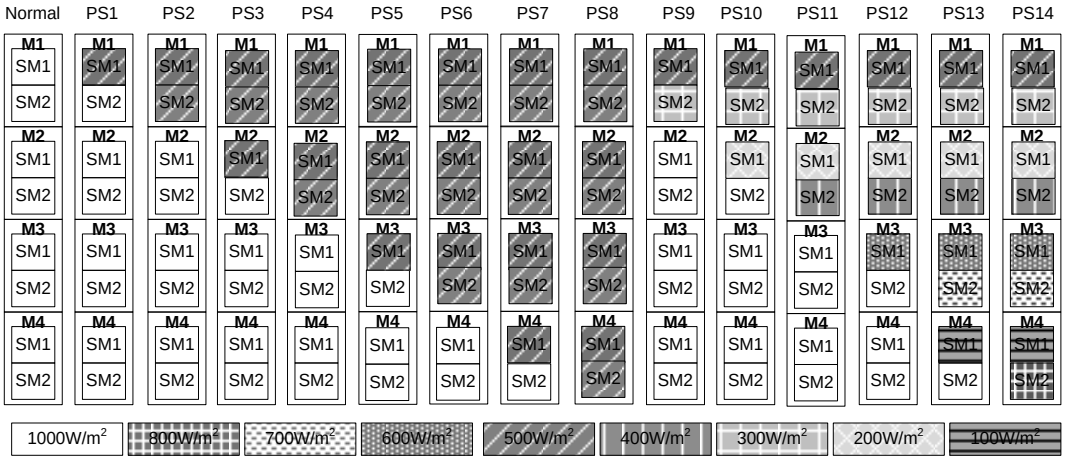

Figure 7. Partial shading conditions

Figure 8 shows the PV system output current, power and voltage for shading conditions PS1 to PS14. The results show that for all partial shading condition, MPP is tracked and power output almost matches with the theoretical power. With proposed SMLDPP PV system power output get improved, and by operating each submodule at its approximate MPP. Also, in the P-V characteristic only one MPP appears, which can get tracked by simple conventional MPPT algorithm. Under shading conditions PV system voltage (Vpv) is maintained almost constant to 124 V, that equalized across all module and submodules of PV string. This shows that all the modules and submodules under any partial condition supply IMPPT current which increases the system power output. Figure 9 show P-V characteristics of PV system under various shading conditions, which shows only one MPP.

The output power generated at submodule level DPP(SMLDPP) is greater than the module level (MLDPP) for nonuniform partial shading conditions over module. For comparison the performance parameters of PV system such as mismatch loss (M_L), conversion efficiency (η_c) and power improvement (ΔP_i) under given partial shadings are calculated using following equations [24], [25]. Mismatch loss (M_L) is the difference between the power generated at unshaded (P_{usd}) and shaded (P_{sd}) conditions for a given technique.

$$\%M_L = \frac{P_{usd}-P_{sd}}{P_{usd}} \times 100 \quad (7)$$

Power conversion efficiency (η_c) is the ratio between power output for shading condition (P_{sd}) to the theoretical power output for same shading (P_{thsd}).

$$\%\eta_c = \frac{P_{sd}}{P_{thsd}} \times 100 \quad (8)$$

Power improvement (ΔP_i) is the percentage change in power employing proposed technique (P_{Pt}) with respect to other technique (P_{ot}).

$$\Delta P_i = \frac{P_{Pt} - P_{ot}}{P_{pt}} \times 100 \quad (9)$$

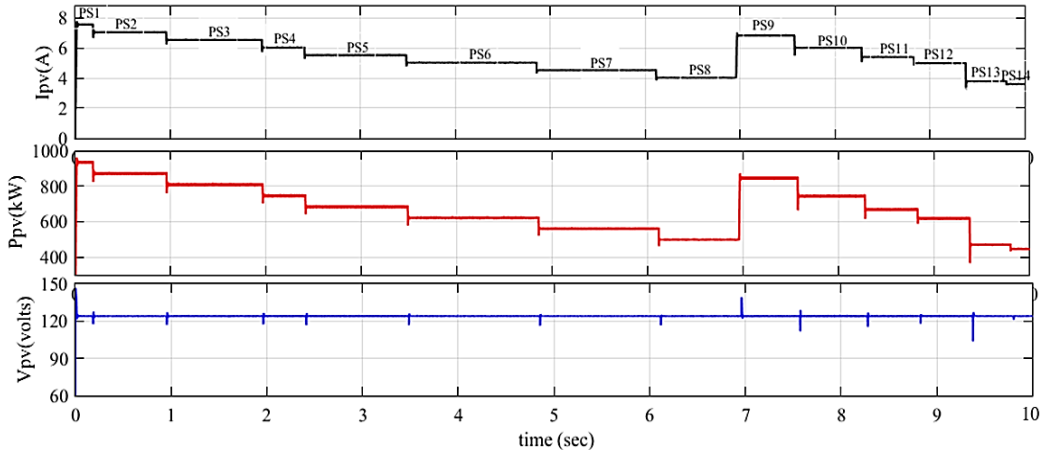

Figure 8. Simulation waveforms I_{pv}, P_{pv}, and V_{pv} for partial shading conditions

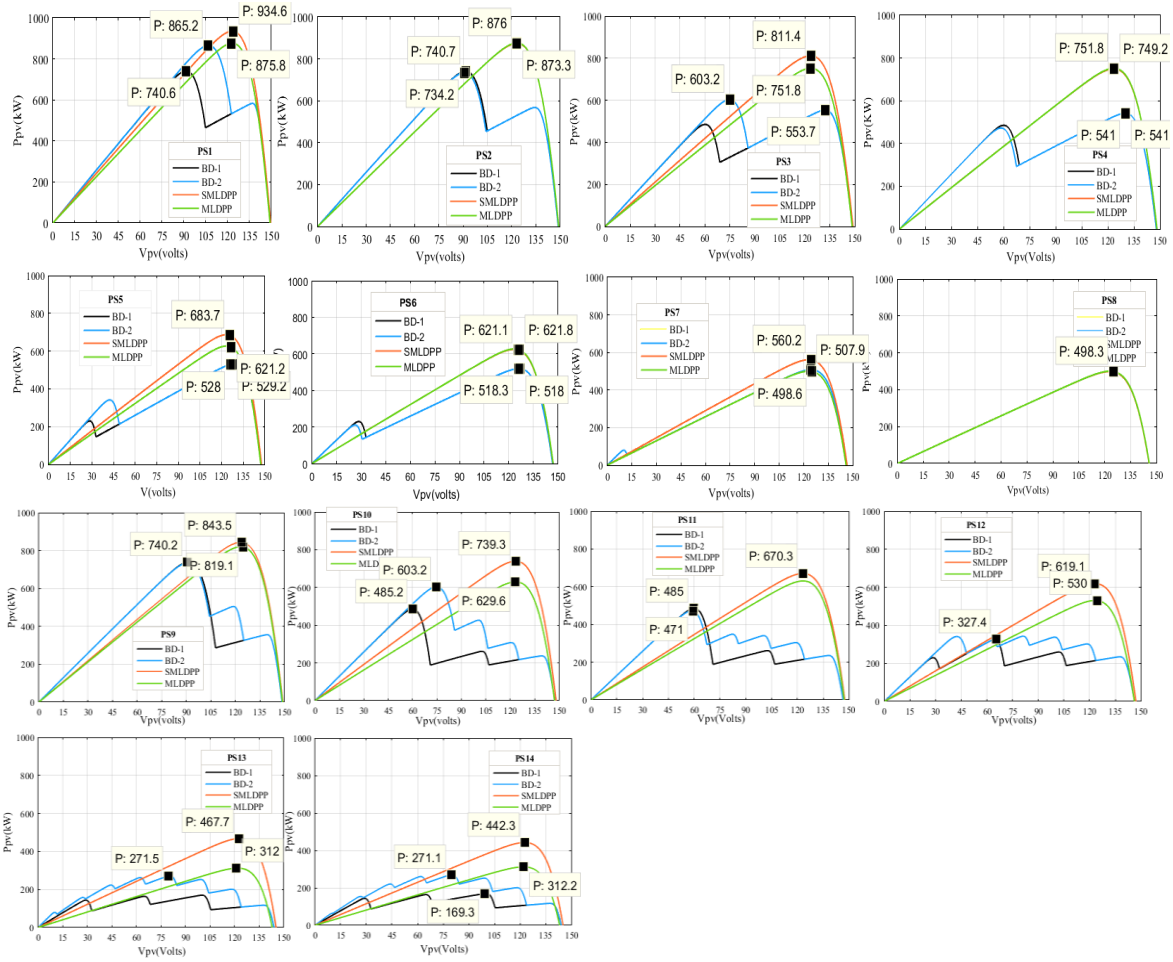

Figure 9. P-V characteristics under partial shading (PS1-PS14) with four mitigation techniques and MPP

It observed from simulation results Table 3 and performance characteristics Figure 10, for PS conditions PS2, PS4, PS6, PS8 the shading is uniform over module, the output power generated by MLDPP and SMLDPP is almost equal, similarly for bypass diode BD-1 and BD-2 are equal. For nonuniform shading conditions between submodules of a modules like PS1, PS3, PS5, PS7, PS9-PS14 the performance of SMDPP is better than other techniques. Mismatch loss is reduced to 1% using SMLDPP technique, with power conversion efficiency of 99%. Power improvement using proposed SMLDPP compared with MLDPP is varies from 5 to 32% under nonuniform shading over a module.

Table 3. Performance parameters under partial shading with different mitigation techniques

Shading	Mitigation Technique	P_{th}(W)	P_{sd} (W)	$\%M_L$ (7)	$\%\eta_c$ (8)	$\%\Delta P_i$ w.r.t. (MLDPP) (9)
PS1	BD-1	937	742	20.81	79.18	-
	BD-2		865	7.68	92.31	-
	MLDPP		871	7.04	92.95	-
	SMLDPP		934	0.32	99.37	6.74
PS2	BD-1	875	742	15.20	84.8	-
	BD-2		734	16.11	83.88	-
	MLDPP		871	0.45	99.54	-
	SMDPP		871	0.45	99.54	0
PS3	BD-1	812	542	33.25	66.74	-
	BD-2		603	25.73	74.26	-
	MLDPP		745	8.25	91.74	-
	SMDPP		808	0.49	99.50	7.79
PS4	BD-1	750	542	27.73	72.26	-
	BD-2		540	28.00	72.00	-
	MLDPP		745	0.66	99.33	-
	SMDPP		745	0.66	99.33	0
PS5	BD-1	687	520	24.3	75.69	-
	BD-2		530	22.85	77.14	-
	MLDPP		621	9.60	90.39	-
	SMDPP		683	0.58	99.41	9.07
PS6	BD-1	625	520	16.80	83.20	-
	BD-2		518	17.12	82.88	-
	MLDPP		621	0.64	99.36	-
	SMDPP		621	0.64	99.36	0
PS7	BD-1	562	500	11.03	88.96	-
	BD-2		508	9.6	90.39	-
	MLDPP		498	0.17	88.61	-
	SMDPP		560	0.35	99.62	11.07
PS8	BD-1	500	498	0.40	99.60	-
	BD-2		498	0.40	99.60	-
	MLDPP		498	0.40	99.60	-
	SMDPP		498	0.40	99.60	0
PS9	BD-1	850	742	12.7	87.29	-
	BD-2		734	13.64	86.35	-
	MLDPP		819	3.64	96.35	-
	SMDPP		845	0.58	99.41	3.07
PS10	BD-1	750	486	35.2	64.80	-
	BD-2		603	19.60	80.40	-
	MLDPP		630	16.00	84.00	-
	SMDPP		743	0.93	99.06	15.30
PS11	BD-1	675	485	28.14	71.85	-
	BD-2		471	30.22	69.77	-
	MLDPP		630	6.66	93.33	-
	SMDPP		670	0.74	99.25	5.97
PS12	BD-1	625	327	94.08	52.32	-
	BD-2		343	45.12	54.88	-
	MLDPP		530	15.20	84.80	-
	SMDPP		620	0.80	99.20	14.51
PS13	BD-1	475	169	64.42	35.57	-
	BD-2		271	42.94	57.05	-
	MLDPP		315	33.68	66.31	-
	SMDPP		470	1.05	98.94	32.97
PS14	BD-1	450	169	62.44	37.55	-
	BD-2		271	39.77	60.22	-
	MLDPP		315	30.00	70.00	-
	SMDPP		445	1.11	98.88	29.21

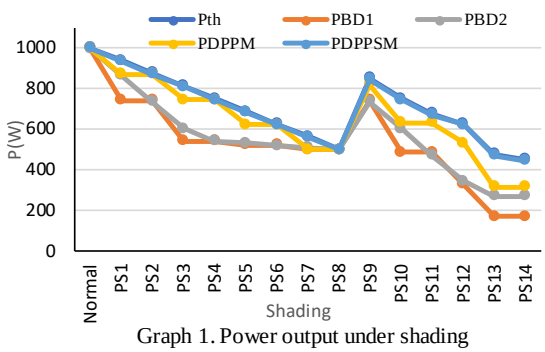

Graph 1. Power output under shading

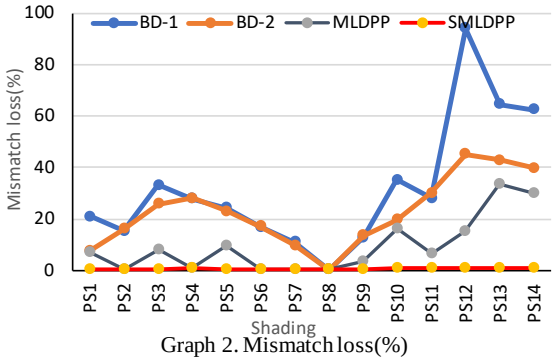

Graph 2. Mismatch loss(%)

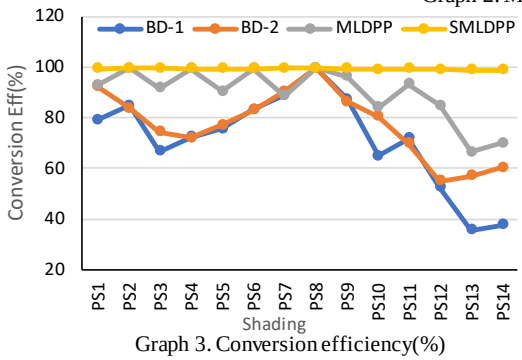

Graph 3. Conversion efficiency(%)

Figure 10. Performance characteristics for various partial shading conditions

4. CONCLUSION

Among the various partial shading mitigation techniques, the proposed SMLDPP technique reduces mismatch loss to 1%. The power conversion efficiency also near to 98-99% which is greater than bypass diode and MLDPP technique for any type shading condition. Power improvement of 5 to 32% over MLDPP justify the increased cost of hardware. This technique is modular and scalable and used for PV module series string with N (=1, 2, 3, …..) number of modules. It operates each module and submodule in series PV string at approximate MPP. Simple to control, scalable to any size of PV string is added advantage of this architecture. The use of soft switching DPP converter further enhance the system efficiency.

REFERENCES

[1] D. Gielen, F. Boshell, D. Saygin, M. D. Bazilian, N. Wagner, and R. Gorini, "The role of renewable energy in the global energy transformation," *Energy Strategy Reviews*, vol. 24, pp. 38–50, 2019, doi: 10.1016/j.esr.2019.01.006.

[2] S. Singer, J.-P. Denruyter, and D. Yener, "The Energy Report: 100% Renewable Energy by 2050," in *Towards 100% Renewable Energy*, 2017, pp. 379–383, doi: 10.1007/978-3-319-45659-1_40.

[3] L. Lin, J. Zhang, and S. Shao, "Differential Power Processing Architecture with Virtual Port Connected in Series and MPPT in Submodule Level," *IEEE Access*, vol. 8, pp. 137897–137909, 2020, doi: 10.1109/ACCESS.2020.3010229.

[4] I. Shams, S. Mekhilef, and K. S. Tey, "Advancement of voltage equalizer topologies for serially connected solar modules as partial shading mitigation technique: A comprehensive review," *Journal of Cleaner Production*, vol. 285, 2021, doi: 10.1016/j.jclepro.2020.124824.

[5] L. F. Lavado Villa, T. P. Ho, J. C. Crebier, and B. Raison, "A power electronics equalizer application for partially shaded photovoltaic modules," *IEEE Transactions on Industrial Electronics*, vol. 60, no. 3, pp. 1179–1190, 2013, doi: 10.1109/TIE.2012.2201431.

[6] H. Jeong, H. Lee, Y. C. Liu, and K. A. Kim, "Review of Differential Power Processing Converter Techniques for Photovoltaic Applications," *IEEE Transactions on Energy Conversion*, vol. 34, no. 1, pp. 351–360, 2019, doi: 10.1109/TEC.2018.2876176.

[7] T. Alves, J. P. N. Torres, R. A. M. Lameirinhas, and C. A. F. Fernandes, "Different techniques to mitigate partial shading in photovoltaic panels," *Energies*, vol. 14, no. 13, 2021, doi: 10.3390/en14133863.

[8] P. S. Shenoy, K. A. Kim, P. T. Krein, and P. L. Chapman, "Differential power processing for efficiency and performance leaps in utility-scale photovoltaics," in *Conference Record of the IEEE Photovoltaic Specialists Conference*, Jun. 2012, pp. 1357–1361, doi: 10.1109/PVSC.2012.6317852.

[9] C. Olalla, C. Deline, D. Clement, Y. Levron, M. Rodriguez, and D. Maksimovic, "Performance of Power-Limited Differential Power Processing Architectures in Mismatched PV Systems," *IEEE Transactions on Power Electronics*, vol. 30, no. 2, pp. 618–631, Feb. 2015, doi: 10.1109/TPEL.2014.2312980.

[10] M. Uno and K. Honda, "Panel-to-Substring Differential Power Processing Converter with Embedded Electrical Diagnosis Capability for Photovoltaic Panels under Partial Shading," *IEEE Transactions on Power Electronics*, vol. 36, no. 9, pp. 10239–10250, 2021, doi: 10.1109/TPEL.2021.3064706.

[11] M. Kasper, S. Herden, D. Bortis, and J. W. Kolar, "Impact of PV string shading conditions on panel voltage equalizing converters and optimization of a single converter system with overcurrent protection," *2014 16th European Conference on Power Electronics and Applications, EPE-ECCE Europe 2014*, 2014, doi: 10.1109/EPE.2014.6910859.
[12] S. Vighetti, Y. Lembeye, J.-P. Ferrieux, and J. Barbaroux, "Photovoltaic module and shadow: study and integration of a current balancing system," *EUPVSEC 2010*, 2010.
[13] F. Wang, T. Zhu, F. Zhuo, H. Yi, and S. Shi, "Submodule level distributed maximum power point tracking PV optimizer with an integrated architecture," *Journal of Power Electronics*, vol. 17, no. 5, pp. 1308–1316, 2017, doi: 10.6113/JPE.2017.17.5.1308.
[14] C. Olalla, D. Clement, M. Rodriguez, and D. Maksimovic, "Architectures and control of submodule integrated dc-dc converters for photovoltaic applications," *IEEE Transactions on Power Electronics*, vol. 28, no. 6, pp. 2980–2997, 2013, doi: 10.1109/TPEL.2012.2219073.
[15] S. Qin, C. B. Barth, and R. C. N. Pilawa-Podgurski, "Enhancing Microinverter Energy Capture with Submodule Differential Power Processing," *IEEE Transactions on Power Electronics*, vol. 31, no. 5, pp. 3575–3585, 2016, doi: 10.1109/TPEL.2015.2464235.
[16] J. T. Stauth, M. D. Seeman, and K. Kesarwani, "Resonant switched-capacitor converters for sub-module distributed photovoltaic power management," *IEEE Transactions on Power Electronics*, vol. 28, no. 3, pp. 1189–1198, 2013, doi: 10.1109/TPEL.2012.2206056.
[17] J. A. A. Qahouq, Y. Jiang, and M. Orabi, "MPPT control and architecture for PV solar panel with sub-module integrated converters," *Journal of Power Electronics*, vol. 14, no. 6, pp. 1281–1292, 2014, doi: 10.6113/JPE.2014.14.6.1281.
[18] H. Luo, H. Wen, X. Li, L. Jiang, and Y. Hu, "Synchronous buck converter based low-cost and high-efficiency sub-module DMPPT PV system under partial shading conditions," *Energy Conversion and Management*, vol. 126, pp. 473–487, 2016, doi: 10.1016/j.enconman.2016.08.034.
[19] J. Jiang, T. Zhang, and D. Chen, "Analysis, Design, and Implementation of a Differential Power Processing DMPPT with Multiple Buck-Boost Choppers for Photovoltaic Module," *IEEE Transactions on Power Electronics*, vol. 36, no. 9, pp. 10214–10223, 2021, doi: 10.1109/TPEL.2021.3063230.
[20] G. Chu, H. Wen, Y. Yang, and Y. Wang, "Elimination of photovoltaic mismatching with improved submodule differential power processing," *IEEE Transactions on Industrial Electronics*, vol. 67, no. 4, pp. 2822–2833, 2020, doi: 10.1109/TIE.2019.2908612.
[21] H. W. Kim, J. H. Park, and H. J. Jeon, "Bidirectional power conversion of isolated switched-capacitor topology for photovoltaic differential power processors," *Journal of Power Electronics*, vol. 16, no. 5, pp. 1629–1638, 2016, doi: 10.6113/JPE.2016.16.5.1629.
[22] C. M. A. Luz, F. L. Tofoli, and E. R. Ribeiro, "Novel differential power processing topology for the mitigation of mismatch in photovoltaic systems," *Electronics Letters*, vol. 58, no. 2, pp. 67–69, 2022, doi: 10.1049/ell2.12364.
[23] G. Chu, H. Wen, Y. Hu, L. Jiang, Y. Yang, and Y. Wang, "Low-Complexity Power Balancing Point-Based Optimization for Photovoltaic Differential Power Processing," *IEEE Transactions on Power Electronics*, vol. 35, no. 10, pp. 10306–10322, 2020, doi: 10.1109/TPEL.2020.2977329.
[24] P. R. Satpathy, T. S. Babu, S. K. Shanmugam, L. N. Popavath, and H. H. Alhelou, "Impact of Uneven Shading by Neighboring Buildings and Clouds on the Conventional and Hybrid Configurations of Roof-Top PV Arrays," *IEEE Access*, vol. 9, pp. 139059–139073, 2021, doi: 10.1109/ACCESS.2021.3118357.
[25] P. R. Satpathy, T. S. Babu, A. Mahmoud, R. Sharma, and B. Nastasi, "A TCT-SC Hybridized Voltage Equalizer for Partial Shading Mitigation in PV Arrays," *IEEE Transactions on Sustainable Energy*, vol. 12, no. 4, pp. 2268–2281, 2021, doi: 10.1109/TSTE.2021.3088687.

BIOGRAPHIES OF AUTHORS

Subhash Murkute currently working as Associate Professor in Department of Electrical Engineering of P.E.S. College of Engineering, Aurangabad, Maharashtra, India. He has completed his under graduate in Electrical, Electronics and Power and Post graduate in Electrical Power System from Government College of Engineering, Aurangabad, Maharashtra in 1997 and 2004 respectively. Pursuing Ph.D. from Dr. Babasaheb Ambedkar Marathwada University, Aurangabad. His main research areas include distributed power generation, power quality, and power electronics converters. He can be contacted at email: murkutes@rediffmail.com.

Vandana Abhay Kulkarni (Deodhar) had joined the institute in 1998 and currently working as Associate Professor in the Department of Electrical Engineering, Government Engineering College Aurangabad. Completed her Ph.D. degree in 2009 at Dr. B.A.M. University Aurangabad. Her current research interests include high-voltage DC transmission system, power system stability, and renewable energy. She can be contacted at email: vandanadk1@gmail.com.